3D geometry and mechanics of a single apical stem cell ensure helically symmetric plant body in multicellular models

Naoya Kamamoto* & Koichi Fujimoto*
*corresponding author

February 2026

Key words: apical stem cell, cell division orientation, Bryophytes, Ferns, least area rule, maximal tension rule, cell mechanics

Abstract

Self-renewing divisions of stem cells at the growing tip universally control plant development. In basal land plants, a single apical stem cell (AC) rotates the division axis by 120 degrees but self-similarly grows to the tetrahedron with three division walls, recapitulating the helically symmetric body architecture. The mechanisms through which geometry and mechanics of AC determine the division axis and its rotation are largely unknown. Here, we developed two 3D multicellular mathematical models to tackle these questions. Our geometrical model reveals that the least area rule, in coordination with the AC surface curvature, is sufficient to drive rotational divisions through the rotation of the AC geometrical proportion. Furthermore, by incorporating the plausible cell growth mechanics, we show that the tetrahedral AC and its rotational division spontaneously emerge from a spherical cell. Notably, we found that the maximal tension rule provides superior robustness against stochastic fluctuation in division orientation compared to the least area rule, as the history of wall formation dictates the tension distribution to guide subsequent divisions. These results suggest that the tetrahedral AC and helically symmetric body plan are natural consequences of self-renewing cell divisions, imposed by 3D geometry and/or mechanics.

1 Introduction

The evolutionary development of the three-dimensional multicellular bodies is the main event for land plants to stand out from their surroundings and flourish on the land (Harrison, 2017; Moody, 2020). Since plant cells cannot rearrange themselves, the appropriate orientation of cell division is crucial for the 3D development (Smolarkiewicz and Dhonukshe, 2013). Basal land plants have only one self-renewing apical stem cell (AC) at their growing tip. Three-dimensional body development is achieved by helically"rotating" the division axis with each cell cycle (Harrison et al., 2009; Véron et al., 2021) (Fig. 1a). This rotational division allocates differentiated daughter cells around the AC. As each daughter subsequently divides to produce a portion of the stem and a leaf (Fig. 1a), rotational division of the AC is indispensable for three-dimensional body organization (Moody, 2020).

The 3D shape of the AC and the pattern of its rotational divisions are closely interrelated. The most common shape is the tetrahedron (Fig. 1a; (Hofmeister, 1868; Crandall-Stotler, 1981; Bower, 1889; Gifford and Foster, 1989; Shaw and Renzaglia, 2004; Dolzblasz et al., 2018; Hasebe, 2020; Cruz and Hetherington, 2025). A tetrahedral AC embedded in the shoot tip has a free surface and three shared walls (Fig. 1a) with the surrounding differentiated tissues. The division wall is inserted parallel to one of these shared walls, resulting in the formation of a tetrahedral AC and a wedge-shaped differentiated cell. This cell (called merophyte) subsequently differentiates to form a leaf and a portion of the stem (Gifford Jr, 1983; Douin, 1925; Korn, 1993; Harrison et al., 2009). The next division wall in the AC is again parallel to one of the shared walls, but the division axis is rotated by 120° from the previous one. The reiteration of such self-renewing, asymmetric cell divisions results in the rotational allocation of differentiated daughters around the AC. The rotational divisions simultaneously maintain the AC geometry as a tetrahedron. This maintenance of a specific geometry may contribute to stem cell maintenance through cell-cell communication, as proposed

for intestinal stem cells in animals (Pentinmikko et al., 2022). Thus, the rotational angle of the division axis in the AC encodes the rotational symmetry of the organ arrangement and consequently the body plan (Gifford Jr, 1983; Douin, 1925; Korn, 1993; Harrison et al., 2009; Véron et al., 2021; Kamamoto et al., 2021). Understanding of this rotation paves the way to elucidating how the early land plants acquired the 3D helically-modular body structure. However, the cellular mechanism by which ACs rotate their division axis remains unclear.

One hypothesis for controlling the rotational division is the least area (Errera's) rule of division plane, which is largely recognized in cell divisions ranging from algae to land plants (Errera, 1886; Berthold, 1886; Thompson, 1942; Cooke and Paolillo Jr, 1980; Miller, 1980; Flanders et al., 1990; Dupuy et al., 2010; Besson and Dumais, 2011; Yoshida et al., 2014; Martinez et al., 2018; Moukhtar et al., 2019; Rong et al., 2022; Ishikawa et al., 2023; Tanaka et al., 2024; Mathew et al., 2025). According to this rule, the division wall of plant cell division follows the minimal interface area between two bubbles inside the mother cell. In the early 20th century, Sir D'Arcy Thompson proposed that the least area rule might govern the arrangement of tetrahedral AC and 120° cells, based on the analogy of his 2D mathematical analysis (Thompson, 1942). The possibility of the least area rule applying to the tetrahedral ACs was also discussed in the observations of fern(Lintilhac and Green, 1976) and lycophyte (Karrfalt, 1977) meristems. Couturier and colleagues elegantly showed that the least area rule (i.e., the shortest geodesic path on a surface) in the meristem, approximated as a conical 2D surface, can generate three types of rotation angle (i.e., 180°, 120°, and 90°) seen in ACs (Couturier et al., 2025). Cammarata and colleagues recently proposed a 3D geometrical model incorporating growth fields and repetitive cell divisions, based on the live-imaging of *Physcomitrium patens* AC. The model quantitatively reproduced the angle of rotational divisions by combining the least area rule with the observed displacement of the centroid (potentially the nucleus) of the division plane away from existing older division walls (Cammarata et al., 2026). Despite the centroid displacement concomitant with an asymmetry of the daughter volume ratio in *P. patens* (Cammarata et al., 2026), the daughter ratio is instead found to be rather symmetrical in many bryophytes, lycophytes, and ferns (Couturier et al., 2025). It is therefore still unclear (1) whether and how the least area rule alone achieves the rotational divisions in broader range of AC 3D geometry (e.g., curvature). The alternative or partially coincident hypothesis is the maximal tension rule. According to this rule, the division wall is set parallel to the maximal tension axis on the mother cell wall, shown at the shoot apex, root wound healing, and cambium of *Arabidopsis thaliana*, where anisotropic mechanical stress driven by tissue geometry is dominant (Louveaux and Hamant, 2013; Hoermayer et al., 2024; Höfler et al., 2024). In cases of low stress anisotropy, the maximal tension rule may align closely with the least area rule(Louveaux and Hamant, 2013; Guérin et al., 2016). However, it remains to be elucidated (2) whether and how the maximal tension rule governs the rotational divisions. Further clarifying (3) the respective advantages of the least area and maximal tension rules could help us to understand their roles in 3D body organization.

Here, we first developed a simple 3D geometrical model to test the least area rule and elucidate the steady-state rotational divisions. Next, we developed an elaborate 3D mechanical multicellular model which revealed that both the least area rule and the maximal tension rule achieve the tetrahedral AC and its helically symmetric division pattern. These results indicate the distinct advantages of each rule in developing 3D body structure under plausible cell geometry and mechanics.

2 Model

2.1 3D Geometrical model for hemispherical meristem

The meristem is modeled as a hemisphere into which a tetrahedral AC is embedded (Fig. 1b). The AC is composed of a spherical free surface and an inner polyhedron, specified by three vertices on the hemispherical surface and one vertex inside the hemisphere (Fig. 1b). To simulate the least area rule, the division plane passing through the mother cell centroid and minimizing the area is searched by uniformly sampling the axis as: $\boldsymbol{n} = (\sin\theta\cos\phi, \sin\theta\sin\phi, \cos\theta)$, where θ and ϕ are polar and azimuthal angles, respectively (Fig. S1 top right). The corresponding axis of the least-area division plane is searched for increments of 1° for both θ and ϕ. After the least area division, the daughter cell with fewer cell vertices is chosen as the next AC. The AC grows until it restores the original volume in an isotropic manner (Fig. S1, right bottom), following observations in early stages of the development (reviewed in (de Keijzer et al., 2021)) and previous

models(Kamamoto et al., 2021; Couturier et al., 2025).

Rotational angle of division direction: The rotational angle is defined as the angle between the outer normals of successive division planes. This angle is measured after projecting these outer normals to the horizontal plane, in a clockwise or counterclockwise direction, following the direction of the rotational divisions.

2.2 3D Mechanical multicellular model

To model plausible cell deformation, growth, and cell division, we employed the triangular biquadratic spring model (TRBS model) (Delingette, 2008), which has been used to plant multicellular modeling (Bozorg et al., 2014; Bonfanti et al., 2023). In the TRBS model, the cell wall is expressed as a mesh of triangular elements (Figs 4a and S3) assuming the hyperelastic material characterized by Young's modulus Y and Poisson's ratio σ (supporting text). At each time step, cell wall deformation was simulated by minimizing the TRBS elastic energy (supporting text) under constant turgor pressure P, then cell wall growth was simulated in a strain-based way as in the previous study (Bonfanti et al., 2023) (supporting text). To simulate indeterminate growth of the meristem, some remeshing operations were introduced, as well as the cell division operation (Figs 4a, S3, and supporting text). Cell growth in merophytes that detach from the AC was not adopted. All the simulations started with a spherical cell with a radius of 10 μm, composed of 162 vertices. We confirmed that the qualitative behavior remained unchanged over a range of parameter values (Y and P; Figs S4 and S5). The simulation was implemented using Julia(Bezanson et al., 2017) and visualized using ParaView(Ahrens et al., 2005).

Maximal tension rule: We introduced the maximal tension rule to the curved free surface of the AC as follows: The cell division axis perpendicular to the division wall is determined to be the axis that best fit perpendicular to both the maximal tension axes of each triangular element and its normal vector. The weighted contribution of each triangular element i is evaluated as the inner product $w_i|\vec{d}\cdot\vec{p_i}|$ where $\vec{d}$ and $\vec{p_i}$ denote the candidate division axis ($|\vec{d}| = 1$) and the normalized minor eigen vector of the second Piola-Kirchhoff stress tensor, respectively. Note that this minor eigenvector is perpendicular to both the major eigenvector and the normal vector of the triangular element. The weight w_i is defined as the product of the triangle area and the eigenvalue of the major axis λ_1, multiplied by the anisotropy $(\lambda_1 - \lambda_2)/\lambda_1$, i.e., $w_i = a_i(\lambda_1 - \lambda_2)$. This weighted contributions from each triangular element are then summed over the AC free surface for each vector $\vec{d}$. The cell division axis is consequently selected as the vector $vecd$ for which this sum is maximized.

AC determination: Following cell division, the next AC is chosen similarly to the geometrical model. To choose the daughter cell with fewer "vertices" as the next AC, the vertices shared by three cells (at free surfaces) and by four cells (at the inner tissue) were regarded as the corresponding AC vertices.

Sustainability of rotational division against orientation fluctuation: After the initial spherical cell had progressed through six cell cycles under the least area rule (e.g., Fig. 3b), we introduced angular fluctuation to rotate the division axis for the next four cell cycles under the least area/maximal tension rules. The magnitude of the angular fluctuation was sampled from circular normal distributions with various standard deviation values (2, 4, 8, 16, and 32 degrees, with 150 samples for each value). The rotation axis was randomly chosen from the plane perpendicular to the division axis. After the simulations, we checked if the AC would sustain the rotational divisions in the same direction as before the imposed fluctuation (Fig. 4g).

3 Results

3.1 Least area rule of cell division plane reproduced 120° rotational divisions in 3D geometrical model

First, we investigate the simplest 3D condition in which an AC is established in a hemispherical meristem. This allows us to examine whether the least area rule of division plane can achieve the self-renewing rotational divisions as a steady state. We initially prepare 3D tri-symmetric tetrahedral AC geometries with a relative height of $\tilde{z_0}$, normalized by the meristem radius (Figs 1b and S1). The least area division plane is numerically determined by comprehensively searching the angles of the division plane passing through the AC centroid in 3D (Fig. S2). After cell division, the tetrahedral daughter is chosen as the next AC (Fig. 1b), and it

grows isotropically to reach the original volume (Fig. S1; Method). We found that the consecutive rotational divisions emerge over a substantial portion of the initial shape (e.g., the polar angle $\geq 40°$ and the cell height > 0.2 in Fig. 1b-c; Video S1). The rotational angle between successive division planes (roughly equivalent to the divergence angle; (Kamamoto et al., 2021)) is approximately 120° (Fig. 1d), as observed in typical leafy liverworts and ferns. Rotational divisions disappear below a threshold of the height-to-meristem radius ratio $\tilde{z_0}$, which is proportional to the curvature of the AC free surface (Fig. 1b). These results show that the least area rule accurately reproduces the rotational divisions when the AC free surface has a sufficient curvature.

3.2 Rotational division is ensured by rotation of geometrical proportion of AC

Since the least area division only depends on the 3D geometry (shape) of AC, we hypothesized that each division would result in the AC geometry rotating. To test this theory, we assessed the geometric similarity of the AC outline proportions before and after division by calculating the similarity of each arc and edge length of the AC outline (Fig. 2a, left). At high curvature, the geometric similarity is maximized when the AC geometry after cell division is compared with the geometry before the cell division under 120° rotation. This rotational self-similarity supports our theory of the rotation of the geometric proportion (Fig. 2a, $\tilde{z_0} = 0.5$). In contrast, at low curvature, the geometric similarity is maximized with no rotation (Fig. 2a, $\tilde{z_0} = 0.05$), which is consistent with the parallel divisions (Fig. 1d). These results indicate that the least area division of the highly curved ACs ensures the rotation of the AC geometrical proportion.

To elucidate whether the curvature-mediated rotation of geometric proportion during each cell cycle leads to the consecutive rotational divisions to a constant direction, we measured the time course of AC geometry using edge and arc lengths (Fig. 2b), given the high curvature of ACs ($\tilde{z_0}$=0.5). Each arc monotonically shortens during multiple rounds of cell cycles (e.g., orange → green → blue circles in Fig. 2b inset), indicating that the arc shared with the youngest and oldest differentiated cells is always the longest and shortest, respectively (Fig. 2b). This exemplifies the consecutive 120° rotation of the AC proportion for each cell cycle. Indeed, the self-similarity is always maximized with 120° rotation to the constant direction (Fig. 2c, magenta plus).

Finally, to understand how the rotation of the AC geometry occurs at high curvature, we analyzed the effect that inserting a least area division wall has on the edge lengths of the AC outline (Fig. 2d, e). At both low and high curvatures, the division wall intersects the longest edge of the AC outline (Fig. 2d, e top-left, blue lines) At low curvature, nevertheless, this edge remains longer than the newly formed edges (Fig. 2d top-right, green and orange lines). Since the next division wall again intersects this longest edge, the division axis is likely to be the same as the previous one (Fig. 2d top-right, magenta). In contrast, at high curvature of the free surface, a newly formed edge (Fig. 2e top-right, green line) increases in length due to the highly curved arc on the free surface (Fig. 2e, top grey curve), and it exceeds the previously longest edge (blue line). This reorders the edge lengths (from Fig. 2e left, blue > green > orange to Fig. 2e right, green > orange > blue), i.e., the rotation of the AC geometry (Fig. 2e, top right). Taken together, these results reveal that the least area division-driven rotational self-similarity ensures the consecutive rotational divisions in 3D.

3.3 Least area rule under plausible cell mechanics establishes tetrahedral AC and the rotational divisions

We next investigated whether the rotational divisions driven by the least area rule function under plausible cell growth and deformation mechanics. To this end, we developed an AC-driven developmental model based on the continuum mechanics-consistent mechanical model (TRBS model, (Delingette, 2008; Bozorg et al., 2014; Bonfanti et al., 2023); Fig. S3). We introduced cell division (Fig. 3a; supporting text) and the indeterminate meristem growth using remeshing algorithms (Fig. S3; supporting text). Both the AC and the adjacent differentiated cells grow through uniform turgor pressure and cell wall extension (Method; (Bonfanti et al., 2023)). The AC specifically divides after reaching a threshold cell volume. At each cell division, the daughter cell with the fewer vertices was chosen as the next AC. Starting the simulation from a single spherical cell, three rounds of symmetric cell division result in a tetrahedral AC geometry (Fig. 3b top row ; Video S2). Subsequent divisions involve inserting the division wall parallel to the oldest division wall surrounding the AC, resulting in consecutive rotational divisions (Fig. 3b bottom row, c; Video S2). The tetrahedral AC and consecutive rotational divisions were reproduced within a certain range of typical cell

wall stiffness and turgor pressure values (Fig. S4, Method). Throughout the simulation time courses, the AC geometry maintains the rotational self-similarity with 120° (Fig. 3d, e), consistent with the hemispherical model (Fig. 2a-c). These results indicate that the establishment of the tetrahedral AC and the maintenance of 120° rotational divisions are natural consequences of the least area division and turgor pressure-driven 3D cell growth.

3.4 Maximal tension rule reproduced 120° rotational divisions ensured by the history of division wall formation

We found that immediately prior to the rotational divisions, the maximal tension pattern as well as the maximal curvatures on the AC free surface tended to align parallel to the future division wall, in accordance with the maximal tension rule (Fig. 3f, g). Therefore, we incorporated the maximal tension rule into the mechanical model (Methods) instead of the least area rule. While this rule does not result in the rotational divisions when applied to the AC free surface and the AC-merophyte shared walls, it does result in rotational divisions when applied to the AC free surface alone (Fig. 4a, S5; Video S3). Unlike simulations with the least area rule, rotational self-similarity of the AC geometry is maintained for several cell cycles at most (Fig. 4b, c). Nevertheless, the rotational divisions continue.

To identify the mechanical properties which ensure the consecutive rotational divisions in the maximal tension rule without requiring the AC self-similarity, we analyze how each division affects the maximal tension pattern. Immediately after each cell division, the maximal tension axes align most closely with the AC-M1 shared wall axis (represented by the normal vector), followed by the axes of the AC-M0 shared wall (formed at the previous division) and the AC-M2 shared wall (Fig. 4d, bottom, inset and top left). As the cell cycle progresses, the maximal tension axes rotate to align with the AC-M0 shared wall axis, while also aligning with the AC-M1 shared wall axis (Fig. 4d bottom, inset and top right). This indicates that the newly formed division wall (i.e., AC-M0 shared wall) pulls the AC free surface inwards, generating the tension pattern aligned with the AC-M0 shared wall axis. As these tension patterns are gradually overwritten by subsequent formation of division walls, at the end of cell cycle, the tension axes align with both the AC-M0 and AC-M1 shared wall axes, but are perpendicular to the AC-M2 shared wall axis (Fig. 4d top right). These results therefore suggest that the history of the division wall formation through transient tensional patterns ensures consecutive rotational divisions even when the AC self-similarity is scarce.

3.5 Maximal tension criterion more robustly maintains the rotational divisions against misorientation

The emergence of rotational divisions by both the least area and the maximal tension rules, but based on different mechanisms (Figs 3b-e and 4a-d), prompted us to identify the distinct advantages of each rule in 3D tissue growth. While the least area rule is advantageous for maintaining the rotational self-similarity (Fig. 3e and 4c), we examined whether the maximal tension rule would be advantageous for increasing the robustness of rotational divisions, mediated by the history of division wall formations. We thus compared how robustly the rotational divisions persist for each orientation rule in the presence of angular fluctuations in the division orientation (Methods). At small fluctuations ($< 10°$ in Fig. 4e) for four cell cycles, both division rules robustly sustain rotational divisions in the same direction before imposing the fluctuation. As fluctuation strength increases, the difference in the probability of sustained rotational divisions between the maximal tension and least area rules became significantly greater, demonstrating that the maximal tension rule more robustly persists rotational divisions than the least area rule (Fig. 4e). These results show that the maximal tension rule ensures rotational sustainability against orientational stochasticity, rather than rotational self-similarity.

4 Discussion

Building on the seminal theoretical study of Couturier and colleagues that meristem angle controls the rotational divisions on a conical 2D surface (Couturier et al., 2025), here we present a 3D geometrical model of the meristem. In this model, the AC is thick and contains an internal node shared by three interfaces, as well as a surface. Incorporating isotropic volumetric growth and cell division following the least area

rule into this geometrical model showed that, consistent with the meristem angle (Couturier et al., 2025), the curvature of AC surface controls the rotational division in 3D, through the rotation of the geometrical proportion of the AC (Fig. 2). Such 3D self-replication with rotation of AC seemingly forms a basis for self-similar growth of plant bodies and organs in modular tissue/organ (i.e., merophyte) arrangement with helical symmetry. Furthermore, our mechanical model showed that such 3D self-replication can be achieved and maintained even under plausible cell growth mechanics (Fig. 3b-e). Therefore, our theoretical results reveal a series of mechanisms that the least area rule and high curvature of surface ensure 3D self-replication leading to the rotational divisions. These factors are testable *in vivo*, by applying the presented or earlier methods (Martinez et al., 2018; Moukhtar et al., 2019; Ishikawa et al., 2023; Tezuka et al., 2025; Cammarata et al., 2026) to 3D volumetric cell data; The least area rule could be verified when the area-minimizing plane passing through the cell centroid (Fig. S2) coincides with the actual division plane. The 3D self-replication could also be confirmed when the presented RMSD takes the minimum between two cell cycles of AC with 120° rotation to a constant direction (as seen in Fig. 2a, c). Investigating these factors in bryophytes and ancestral algae in future experiments would elucidate the design principle behind the development of 3D body symmetry from 1D or 2D cell arrangements during land plant evolution.

Moreover, our mechanical model (Fig. 3f, g, and 4a) revealed that the maximal tension pattern on the AC surface enables the rotational division. In the maximal tension rule, rotational divisions were ensured by the iterative deformation of the AC surface by the formation of division walls (Fig. 4d). The surface around the fringe of the division wall is pulled inward mechanically, resulting in the emergence of correlated steep curvature and tension towards the division wall (Figs 3f and 4d). Therefore, the curvature pattern on the surface could indicate the maximal tension rule and help to predict the division plane *in vivo*. Such a tension pattern is partially overwritten by the subsequent division wall formation (Fig. 4d). Thus, once AC with three shared walls is established, the total tension pattern aligns toward the newer walls (AC-M0 and AC-M1 shared walls) (Fig. 4d). In this way, the next division wall is always set parallel to the AC-M2 shared wall, resulting in rotational division. Importantly, the rotational division mediated by the history of division wall formation is more robust against fluctuation in the division axis than the division mediated by the geometrical self-similarity under the least area rule (Fig. 4e). This is because such fluctuation little affects the tension pattern on the surface around the fringe of the newly formed division wall but causes aberrant rotation or non-rotation of the geometrical proportion of AC. Taken together with the redundant processes regulating cell division orientation *in vivo* (Uyehara and Rasmussen, 2023), the maximal tension and the least area rule may contribute to spindle orientation and refining the exact direction by minimizing the division wall area, respectively, thereby cooperatively achieving cell division.

The cell-based representation of our mechanical model (Figs 3a and S3) enables us to incorporate various cytological regulators of cell division, growth, and differentiation, including the gene regulatory networks, PIN-mediated polar transport of auxin (Yoshida et al., 2014), plasmodesmata (Abitbol-Spangaro et al., 2025), microtubules (Bozorg et al., 2014), and nuclear displacement (Robinson et al., 2011; Cammarata et al., 2026). The fine 3D cell geometry, repetitive cell divisions, and stress patterns (presented in Figs 3b, c, f, and 4a) could simulate the morphogenesis of multicellular and multilayered plant bodies and organs that originate from one or a few cells. One promising area for future research is the alternative rotation angle (e.g., 180°), which has been observed in bryophytes and ferns, and predicted under the steep meristem angle in the conical surface model (Couturier et al., 2025). If the least area rule in 3D could reproduce the 180° rotation angle, such curvature of meristem is probably steeper than both the spherical surface (Fig. 1b) and some deviation from the spherical surface due to cell-cell adjacent topology and geometry of both AC and surrounding merophytes (Figs 3b, c, and S4). Such a steep AC surface may be enhanced by tip growth or cortical microtubule-driven anisotropic diffuse growth of the AC (Ren et al., 2017). Alternatively, the maximum tension division may reproduce such a rotation angle without a visible steep surface in the AC, but due to anisotropic stress state imposed by that of surrounding merophytes, which is further caused by cortical microtubules-mediated dorsoventrality or flatness of organs (Shaw and Renzaglia, 2004; Plackett et al., 2015; Cruz and Hetherington, 2025). Thus, extending the present model by incorporating the corresponding cell growth anisotropy (e.g., tip growth (Dumais et al., 2003; Kang et al., 2024) and/or ordering the cortical microtubules (Bozorg et al., 2014; Zhao et al., 2020)) would modulate the rotational angles.

Another future extension is to explain rotational divisions in the root apical meristem in lycophytes and ferns. In addition to anticlinal rotational divisions against a distal cell wall, periclinal divisions also occur to produce the root cap (Imaichi and Kato, 1989; Aragón-Raygoza et al., 2020). Since the periclinal division

plane only intersects the sidewalls, the cue for division orientation is likely to follow the tension on these sidewalls. Incorporating this sidewall tension pattern would clarify the contribution of each sidewall and the distal wall to the mechanical switching of the division pattern. This analysis may, in turn, lead to the developmental switching from aerial to subterranean organs.

Other future extension is to account for the early embryonic development, in which the tetrahedral cells typically originate from a single spherical apical cell (Fig. 3b) in angiosperms (Gifford and Foster, 1989; Dresselhaus and Jürgens, 2021). The emergence of such tetrahedral cells has been shown to be regulated by the least area rule in Arabidopsis embryo(Yoshida et al., 2014; Moukhtar et al., 2019), whereas the division plane has been reported to deviate from the least area plane in rice embryo (Tezuka et al., 2025). The presented emergence of tetrahedral cells by the maximal tension divisions (Fig. 4) provides a potential mechanism. Incorporating the tissue geometry surrounding various angiosperm embryos into our model will enable us to test whether the maximal tension or least area rule accounts for the early embryogenesis. These future extensions of the present model would predict the potential regulatory factors in the conservation and diversification of plant morphogenesis driven by a small number of cells.

5 Acknowledgements

We thank Masaki Shimamura (Hiroshima University, Japan), Satoru Tsugawa (Akita Pref. University, Japane) and Minako Ueda (Tohoku Universitu, Japan) for valuable discussions and suggestions. This work is supported by the Japan Science and Technology Agency (CREST [JPMJCR2121 to N.K. and K.F.]).

6 Author contributions

NK and KF conceived and designed the research. NK developed the mathematical models, wrote the code, and performed the simulations. NK and KF wrote the manuscript.

References

Jeanne Abitbol-Spangaro, Gladys Cloarec, Arthur Muller, Stéphanie Hallet, Claire Boulogne, Cynthia Gillet, Vojtěch Schmidt, Petre I. Dobrev, Roman Skokan, Valentin Couvreur, Jeroen de Keijzer, Christophe Godin, and Yoan Coudert. Robust branch patterning in moss shoots via symplasmic auxin diffusion. *Current Biology*, 35(21):5238–5251.e10, November 2025. ISSN 0960-9822. doi: 10.1016/j.cub.2025.09.031. URL `https://www.cell.com/current-biology/abstract/S0960-9822(25)01201-1`.

James Ahrens, Berk Geveci, and Charles Law. ParaView: An End-User Tool for Large-Data Visualization. In *Visualization Handbook*, volume 717, pages 717–731. Butterworth-Heinemann, January 2005. doi: 10.1016/B978-012387582-2/50038-1. URL `https://www.sciencedirect.com:5037/science/chapter/edited-volume/abs/pii/B9780123875822500381`.

Alejandro Aragón-Raygoza, Alejandra Vasco, Ikram Blilou, Luis Herrera-Estrella, and Alfredo Cruz-Ramírez. Development and Cell Cycle Activity of the Root Apical Meristem in the Fern Ceratopteris richardii. *Genes*, 11(12):1455, December 2020. ISSN 2073-4425. doi: 10.3390/genes11121455. URL `https://www.mdpi.com/2073-4425/11/12/1455`.

Gottfried Berthold. *Studien über protoplasmamechanik*. Arthur Felix Verlag, Leipzig, 1886.

Sébastien Besson and Jacques Dumais. Universal rule for the symmetric division of plant cells. *Proceedings of the National Academy of Sciences*, 108(15):6294–6299, April 2011. doi: 10.1073/pnas.1011866108. URL `https://www.pnas.org/doi/10.1073/pnas.1011866108`.

Jeff Bezanson, Alan Edelman, Stefan Karpinski, and Viral B. Shah. Julia: A Fresh Approach to Numerical Computing. *SIAM Review*, 59(1):65–98, January 2017. ISSN 0036-1445. doi: 10.1137/141000671. URL `https://epubs.siam.org/doi/10.1137/141000671`. Publisher: Society for Industrial and Applied Mathematics.

Alessandra Bonfanti, Euan Thomas Smithers, Matthieu Bourdon, Alex Guyon, Philip Carella, Ross Carter, Raymond Wightman, Sebastian Schornack, Henrik Jönsson, and Sarah Robinson. Stiffness transitions in new walls post-cell division differ between *Marchantia polymorpha* gemmae and *Arabidopsis thaliana* leaves. *Proceedings of the National Academy of Sciences*, 120(41):e2302985120, October 2023. doi: 10.1073/pnas.2302985120. URL https://www.pnas.org/doi/full/10.1073/pnas.2302985120.

Frederick Orpen Bower. The comparative examination of the meristems of Ferns, as a Phylogenetic Study. *Annals of Botany*, os-3(3):305–392, August 1889. ISSN 0305-7364. doi: 10.1093/oxfordjournals.aob.a089998. URL https://doi.org/10.1093/oxfordjournals.aob.a089998.

Behruz Bozorg, Pawel Krupinski, and Henrik Jönsson. Stress and Strain Provide Positional and Directional Cues in Development. *PLOS Computational Biology*, 10(1):e1003410, January 2014. ISSN 1553-7358. doi: 10.1371/journal.pcbi.1003410. URL https://journals.plos.org/ploscompbiol/article?id=10.1371/journal.pcbi.1003410.

Joseph Cammarata, Sören Strauss, Brendan Lane, Robert Kelly-Bellow, Laure Mancini, Teva Vernoux, Yoan Coudert, Adrienne H. K. Roeder, and Richard S. Smith. Spiral phyllotaxis in the moss Physcomitrium patens emerges from simple division rules of the apical cell. *Current Biology*, 0(0), February 2026. ISSN 0960-9822. doi: 10.1016/j.cub.2026.01.059. URL https://www.cell.com/current-biology/abstract/S0960-9822(26)00133-8.

T. J. Cooke and D. J. Paolillo Jr. The Control of the Orientation of Cell Divisions in Fern Gametophytes. *American Journal of Botany*, 67(9):1320–1333, 1980. ISSN 1537-2197. doi: 10.1002/j.1537-2197.1980.tb07764.x. URL https://onlinelibrary.wiley.com/doi/abs/10.1002/j.1537-2197.1980.tb07764.x.

Étienne Couturier, Paula Llanos, Antoine Lizée, Sébastien Besson, and Jacques Dumais. The self-replicating cellular organization of shoot apical meristems. *American Journal of Botany*, 112(4):e70027, 2025. ISSN 1537-2197. doi: 10.1002/ajb2.70027. URL https://onlinelibrary.wiley.com/doi/abs/10.1002/ajb2.70027.

B Crandall-Stotler. Morphology/anatomy of Hepaticae and Anthocerotae. *Advance in Bryology*, 1:315–398, 1981.

Rafael Cruz and Alexander J. Hetherington. Identification of a tetrahedral apical cell preserved within a fossilized fern fiddlehead. *Current Biology*, 35(2):383–390.e2, January 2025. ISSN 0960-9822. doi: 10.1016/j.cub.2024.10.076. URL https://www.sciencedirect.com/science/article/pii/S0960982224015033.

Jeroen de Keijzer, Alejandra Freire Rios, and Viola Willemsen. *Physcomitrium patens*: A Single Model to Study Oriented Cell Divisions in 1D to 3D Patterning. *International Journal of Molecular Sciences*, 22(5):2626, January 2021. ISSN 1422-0067. doi: 10.3390/ijms22052626. URL https://www.mdpi.com/1422-0067/22/5/2626.

Hervé Delingette. Biquadratic and Quadratic Springs for Modeling St Venant Kirchhoff Materials. In Fernando Bello and P. J. Eddie Edwards, editors, *Biomedical Simulation*, Lecture Notes in Computer Science, pages 40–48, Berlin, Heidelberg, 2008. Springer. ISBN 9783540705215. doi: 10.1007/978-3-540-70521-5_5.

Alicja Dolzblasz, Elżbieta Myśkow, and Edyta M. Gola. Meristems of Seedless Vascular Plants: The State of the Art. In Helena Fernández, editor, *Current Advances in Fern Research*, pages 47–73. Springer International Publishing, Cham, 2018. ISBN 9783319751030. doi: 10.1007/978-3-319-75103-0_3. URL https://doi.org/10.1007/978-3-319-75103-0_3.

Ch Douin. La theorie des initiales chez les hepatiques à feuilles. *Bull Soc Bot Fr*, 72(3):565–591, 1925.

Thomas Dresselhaus and Gerd Jürgens. Comparative Embryogenesis in Angiosperms: Activation and Patterning of Embryonic Cell Lineages. *Annual Review of Plant Biology*, 72(Volume 72, 2021):641–676, June 2021. ISSN 1543-5008, 1545-2123. doi: 10.1146/annurev-arplant-082520-094112. URL https://www.annualreviews.org/content/journals/10.1146/annurev-arplant-082520-094112. Publisher: Annual Reviews.

Jacques Dumais, Sidney L. Shaw, Charles R. Steele, Sharon R. Long, and Peter M. Ray. An anisotropic-viscoplastic model of plant cell morphogenesis by tip growth. *International Journal of Developmental Biology*, 50(2-3):209–222, January 2003. ISSN 0214-6282, 1696-3547. doi: 10.1387/ijdb.052066jd. URL http://www.ijdb.ehu.es/web/paper/052066jd.

Lionel Dupuy, Jonathan Mackenzie, and Jim Haseloff. Coordination of plant cell division and expansion in a simple morphogenetic system. *Proceedings of the National Academy of Sciences*, 107(6):2711–2716, February 2010. doi: 10.1073/pnas.0906322107. URL https://www.pnas.org/doi/10.1073/pnas.0906322107.

L. Errera. Sur une condition fondamentale d' equilibre des cellules vivantes, 1886. URL https://cir.nii.ac.jp/crid/1370861707360109572.

D J Flanders, D J Rawlins, P J Shaw, and C W Lloyd. Nucleus-associated microtubules help determine the division plane of plant epidermal cells: avoidance of four-way junctions and the role of cell geometry. *Journal of Cell Biology*, 110(4):1111–1122, April 1990. ISSN 0021-9525. doi: 10.1083/jcb.110.4.1111. URL https://doi.org/10.1083/jcb.110.4.1111.

Ernest M. Gifford and Adriance S. Foster. *Morphology and Evolution of Vascular Plants*. W. H. FREEMAN AND COMPANY, New York, and Basingstoke, February 1989.

EM Gifford Jr. Concept of apical cells in bryophytes and pteridophytes. *Annu Rev Plant Physiol*, 34(1): 419–440, 1983.

Adrien Guérin, Simon Gravelle, and Jacques Dumais. Forces behind plant cell division. *Proceedings of the National Academy of Sciences*, 113(32):8891–8893, August 2016. doi: 10.1073/pnas.1609309113. URL https://www.pnas.org/doi/full/10.1073/pnas.1609309113.

C Jill Harrison. Development and genetics in the evolution of land plant body plans. *Phil Trans R Soc B*, 372(1713):20150490, 2017.

C. Jill Harrison, Adrienne H. K. Roeder, Elliot M. Meyerowitz, and Jane A. Langdale. Local Cues and Asymmetric Cell Divisions Underpin Body Plan Transitions in the Moss *Physcomitrella patens*. *Current Biology*, 19(6):461–471, March 2009. ISSN 0960-9822. doi: 10.1016/j.cub.2009.02.050. URL https://www.cell.com/current-biology/abstract/S0960-9822(09)00803-3.

Mitsuyasu Hasebe. *Morphology and Evolution of Land Plants*. Shokabo, Tokyo, July 2020. ISBN 978-4-7853-5871-6.

Lukas Hoermayer, Juan Carlos Montesinos, Nicola Trozzi, Leonhard Spona, Saiko Yoshida, Petra Marhava, Silvia Caballero-Mancebo, Eva Benková, Carl-Philip Heisenberg, Yasin Dagdas, Mateusz Majda, and Jiří Friml. Mechanical forces in plant tissue matrix orient cell divisions via microtubule stabilization. *Developmental Cell*, 59(10):1333–1344.e4, May 2024. ISSN 1534-5807. doi: 10.1016/j.devcel.2024.03.009. URL https://www.cell.com/developmental-cell/abstract/S1534-5807(24)00177-1.

Wilhelm Hofmeister. *Allgemeine morphologie der Gewächse*. Engelmann, Leipzig, 1868.

Mathias Höfler, Xiaomin Liu, Thomas Greb, and Karen Alim. Mechanical forces instruct division plane orientation of cambium stem cells during radial growth in *Arabidopsis thaliana*. *Current Biology*, 34(23): 5518–5531.e4, December 2024. ISSN 0960-9822. doi: 10.1016/j.cub.2024.10.046. URL https://www.cell.com/current-biology/abstract/S0960-9822(24)01441-6.

Ryoko Imaichi and Masahiro Kato. Developmental anatomy of the shoot apical cell, rhizophore and root ofSelaginella uncinata. *The botanical magazine = Shokubutsu-gaku-zasshi*, 102(3):369–380, September 1989. ISSN 1618-0860. doi: 10.1007/BF02488120. URL https://doi.org/10.1007/BF02488120.

Masaki Ishikawa, Ayaka Fujiwara, Ken Kosetsu, Yuta Horiuchi, Naoya Kamamoto, Naoyuki Umakawa, Yosuke Tamada, Liechi Zhang, Katsuyoshi Matsushita, Gergo Palfalvi, Tomoaki Nishiyama, Sota Kitasaki, Yuri Masuda, Yoshiki Shiroza, Munenori Kitagawa, Toru Nakamura, Hongchang Cui, Yuji Hiwatashi, Yukiko Kabeya, Shuji Shigenobu, Tsuyoshi Aoyama, Kagayaki Kato, Takashi Murata, Koichi Fujimoto,

Philip N. Benfey, Mitsuyasu Hasebe, and Rumiko Kofuji. GRAS transcription factors regulate cell division planes in moss overriding the default rule. *Proceedings of the National Academy of Sciences*, 120(4): e2210632120, January 2023. doi: 10.1073/pnas.2210632120. URL https://www.pnas.org/doi/10.1073/pnas.2210632120.

Naoya Kamamoto, Taishi Tano, Koichi Fujimoto, and Masaki Shimamura. Rotation angle of stem cell division plane controls spiral phyllotaxis in mosses. *Journal of Plant Research*, 134(3):457–473, May 2021. ISSN 1618-0860. doi: 10.1007/s10265-021-01298-0. URL https://doi.org/10.1007/s10265-021-01298-0.

Zichen Kang, Tomonobu Nonoyama, Yukitaka Ishimoto, Hikari Matsumoto, Sakumi Nakagawa, Minako Ueda, and Satoru Tsugawa. A viscoelastic–plastic deformation model of hemisphere-like tip growth in Arabidopsis zygotes. *Quantitative Plant Biology*, 5:e13, January 2024. ISSN 2632-8828. doi: 10.1017/qpb.2024.13. URL https://www.cambridge.org/core/journals/quantitative-plant-biology/article/viscoelasticplastic-deformation-model-of-hemispherelike-tip-growth-in-arabidopsis-zygotes/659C0F1BC918E07CFA478BE33F242734.

Eric E. Karrfalt. An Apical Cell in the Shoot Apex of Isoëtes tuckermanii. *American Fern Journal*, 67(3): 68–72, 1977. ISSN 0002-8444. doi: 10.2307/1546767. URL https://www.jstor.org/stable/1546767.

Robert W Korn. Apical cells as meristems. *Acta Biotheor*, 41(3):175–189, 1993.

Philip M. Lintilhac and Paul B. Green. Patterns of Microfibrillar Order in a Dormant Fern Apex. *American Journal of Botany*, 63(6):726–728, 1976. ISSN 1537-2197. doi: 10.1002/j.1537-2197.1976.tb11862.x. URL https://onlinelibrary.wiley.com/doi/abs/10.1002/j.1537-2197.1976.tb11862.x.

Marion Louveaux and Olivier Hamant. The mechanics behind cell division. *Current Opinion in Plant Biology*, 16(6):774–779, December 2013. ISSN 1369-5266. doi: 10.1016/j.pbi.2013.10.011. URL https://www.sciencedirect.com/science/article/pii/S136952661300160X.

Pablo Martinez, Lindy A. Allsman, Kenneth A. Brakke, Christopher Hoyt, Jordan Hayes, Hong Liang, Wesley Neher, Yue Rui, Allyson M. Roberts, Amir Moradifam, Bob Goldstein, Charles T. Anderson, and Carolyn G. Rasmussen. Predicting Division Planes of Three-Dimensional Cells by Soap-Film Minimization. *The Plant Cell*, 30(10):2255–2266, October 2018. ISSN 1040-4651. doi: 10.1105/tpc.18.00401. URL https://doi.org/10.1105/tpc.18.00401.

Mabel Maria Mathew, Jeroen Saccheri, Srijan Das, Kreedika Rajagopalan, Brendan Lane, Sidhardh Ka, Richard S. Smith, Viola Willemsen, Monica L. Garcia Gomez, Bandan Chakrabortty, Ben Scheres, Kirsten Ten Tusscher, and Kalika Prasad. Wound repair in plants guided by cell geometry. *Current Biology*, 0(0), July 2025. ISSN 0960-9822. doi: 10.1016/j.cub.2025.06.072. URL https://www.cell.com/current-biology/abstract/S0960-9822(25)00860-7.

John H. Miller. Orientation of the Plane of Cell Division in Fern Gametophytes: The Roles of Cell Shape and Stress. *American Journal of Botany*, 67(4):534–542, 1980. ISSN 0002-9122. doi: 10.2307/2442293. URL https://www.jstor.org/stable/2442293.

Laura A Moody. Three-dimensional growth: a developmental innovation that facilitated plant terrestrialization. *J Plant Res*, pages 1–8, 2020.

Julien Moukhtar, Alain Trubuil, Katia Belcram, David Legland, Zhor Khadir, Aurélie Urbain, Jean-Christophe Palauqui, and Philippe Andrey. Cell geometry determines symmetric and asymmetric division plane selection in Arabidopsis early embryos. *PLoS computational biology*, 15(2):e1006771, 2019.

Nalle Pentinmikko, Rodrigo Lozano, Sandra Scharaw, Simon Andersson, Johanna I. Englund, David Castillo-Azofeifa, Aaron Gallagher, Martin Broberg, Ki-Young Song, Agustín Sola Carvajal, Alessondra T. Speidel, Michael Sundstrom, Nancy Allbritton, Molly M. Stevens, Ophir D. Klein, Ana Teixeira, and Pekka Katajisto. Cellular shape reinforces niche to stem cell signaling in the small intestine. *Science Advances*, 8(41): eabm1847, October 2022. doi: 10.1126/sciadv.abm1847. URL https://www.science.org/doi/10.1126/sciadv.abm1847.

Andrew RG Plackett, Verónica S Di Stilio, and Jane A Langdale. Ferns: the missing link in shoot evolution and development. *Front Plant Sci*, 6:972, 2015.

Huibo Ren, Xie Dang, Xianzhi Cai, Peihang Yu, Yajun Li, Shanshan Zhang, Menghong Liu, Binqing Chen, and Deshu Lin. Spatio-temporal orientation of microtubules controls conical cell shape in Arabidopsis thaliana petals. *PLOS Genetics*, 13(6):e1006851, June 2017. ISSN 1553-7404. doi: 10.1371/journal.pgen.1006851. URL `https://journals.plos.org/plosgenetics/article?id=10.1371/journal.pgen.1006851`.

Sarah Robinson, Pierre Barbier de Reuille, Jordi Chan, Dominique Bergmann, Przemyslaw Prusinkiewicz, and Enrico Coen. Generation of Spatial Patterns Through Cell Polarity Switching. *Science*, 333(6048): 1436–1440, September 2011. doi: 10.1126/science.1202185. URL `https://www.science.org/doi/full/10.1126/science.1202185`.

Duoyan Rong, Shuai Zhao, Wenxin Tang, Nan Luo, Hai He, Zhuqing Wang, Huimin Ma, Yimei Huang, Xiaoxun Yao, Xue Pan, Lin Lv, Jiajing Xiao, Renyi Liu, Shingo Nagawa, and Chizuko Yamamuro. ROP signaling regulates spatial pattern of cell division and specification of meristem notch. *Proceedings of the National Academy of Sciences*, 119(47):e2117803119, November 2022. doi: 10.1073/pnas.2117803119. URL `https://www.pnas.org/doi/10.1073/pnas.2117803119`.

Jonathan Shaw and Karen Renzaglia. Phylogeny and diversification of bryophytes. *American Journal of Botany*, 91(10):1557–1581, 2004. ISSN 1537-2197. doi: 10.3732/ajb.91.10.1557. URL `https://onlinelibrary.wiley.com/doi/abs/10.3732/ajb.91.10.1557`.

Michalina Smolarkiewicz and Pankaj Dhonukshe. Formative Cell Divisions: Principal Determinants of Plant Morphogenesis. *Plant and Cell Physiology*, 54(3):333–342, March 2013. ISSN 0032-0781. doi: 10.1093/pcp/pcs175. URL `https://doi.org/10.1093/pcp/pcs175`.

Sayuri Tanaka, Yuuki Matsushita, Yuga Hanaki, Takumi Higaki, Naoya Kamamoto, Katsuyoshi Matsushita, Tetsuya Higashiyama, Koichi Fujimoto, and Minako Ueda. HD-ZIP IV genes are essential for embryo initial cell polarization and the radial axis formation in *Arabidopsis*. *Current Biology*, 34(20):4639–4649.e4, October 2024. ISSN 0960-9822. doi: 10.1016/j.cub.2024.08.038. URL `https://www.cell.com/current-biology/abstract/S0960-9822(24)01153-9`.

Moeno Tezuka, Takunori Kitta, Haruka Kumakura, Moeko Sato, Naoya Kamamoto, Satoshi Naramoto, Hiroyuki Tsuji, Takashi Okamoto, and Atsuko Kinoshita. 3D Imaging Reveals Robustness and Plasticity of Cell Division in Rice Early Embryogenesis. *Plant and Cell Physiology*, page pcaf171, December 2025. ISSN 1471-9053. doi: 10.1093/pcp/pcaf171. URL `https://doi.org/10.1093/pcp/pcaf171`.

D'Arcy Wentworth Thompson. *On growth and form*. Cambridge University Press, UK, second edition, 1942.

Aimee N. Uyehara and Carolyn G. Rasmussen. Redundant mechanisms in division plane positioning. *European Journal of Cell Biology*, 102(2):151308, June 2023. ISSN 0171-9335. doi: 10.1016/j.ejcb.2023.151308. URL `https://www.sciencedirect.com/science/article/pii/S0171933523000237`.

Elsa Véron, Teva Vernoux, and Yoan Coudert. Phyllotaxis from a Single Apical Cell. *Trends in Plant Science*, 26(2):124–131, February 2021. ISSN 1360-1385. doi: 10.1016/j.tplants.2020.09.014. URL `https://www.sciencedirect.com/science/article/pii/S1360138520302922`.

Saiko Yoshida, Pierre Barbier de Reuille, Brendan Lane, George W Bassel, Przemyslaw Prusinkiewicz, Richard S Smith, and Dolf Weijers. Genetic control of plant development by overriding a geometric division rule. *Dev Cell*, 29(1):75–87, 2014.

Feng Zhao, Fei Du, Hadrien Oliveri, Lüwen Zhou, Olivier Ali, Wenqian Chen, Shiliang Feng, Qingqing Wang, Shouqin Lü, Mian Long, René Schneider, Arun Sampathkumar, Christophe Godin, Jan Traas, and Yuling Jiao. Microtubule-Mediated Wall Anisotropy Contributes to Leaf Blade Flattening. *Current Biology*, 30(20):3972–3985.e6, October 2020. ISSN 0960-9822. doi: 10.1016/j.cub.2020.07.076. URL `https://www.sciencedirect.com/science/article/pii/S0960982220311015`.

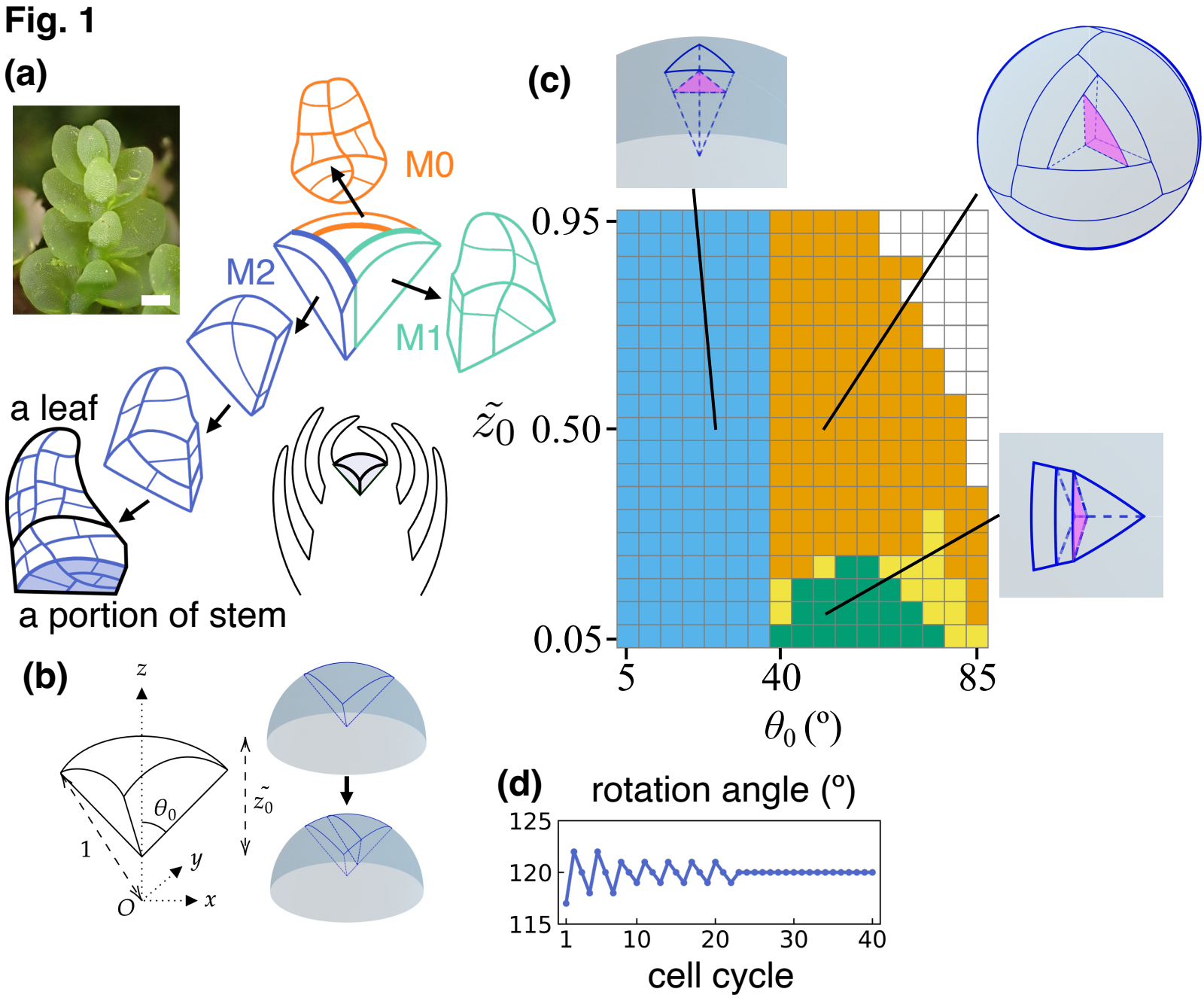

Fig. 1

The least area rule governs rotational divisions in the geometrical model.

(a) Schematics of the tetrahedral AC, merophyte (M0, M1, M2: labeled in order of the time since cell division from AC), and the corresponding helically symmetric lateral organ arrangement in the leafy liverwort *Haplomitrium mnioides*. The photo was taken at Nichinan, Miyazaki, Japan. Bar: 1 mm.

(b) Hemispherical geometric model. The initial shape of tri-symmetric AC is represented as two parameters: polar angle θ_0 and dimensionless cell height ($\tilde{z}_0$) relative to the meristem radius. The division plane is chosen as it passes through the AC centroid and minimizes the area. After division, the daughter with a smaller number of cell vertices is chosen as the next AC, and it isotropically grows to the original cell volume.

(c) Phase diagram of simulated division patterns for various θ_0 and $\tilde{z}_0$. Rotational divisions (orange, top right inset); periclinal division (blue, top left inset); parallel divisions (green, right bottom inset); inconclusive region (yellow).

(d) Time course of the rotation angle at $\theta_0 = 50^\circ$ and $\tilde{z}_0 = 0.5$.

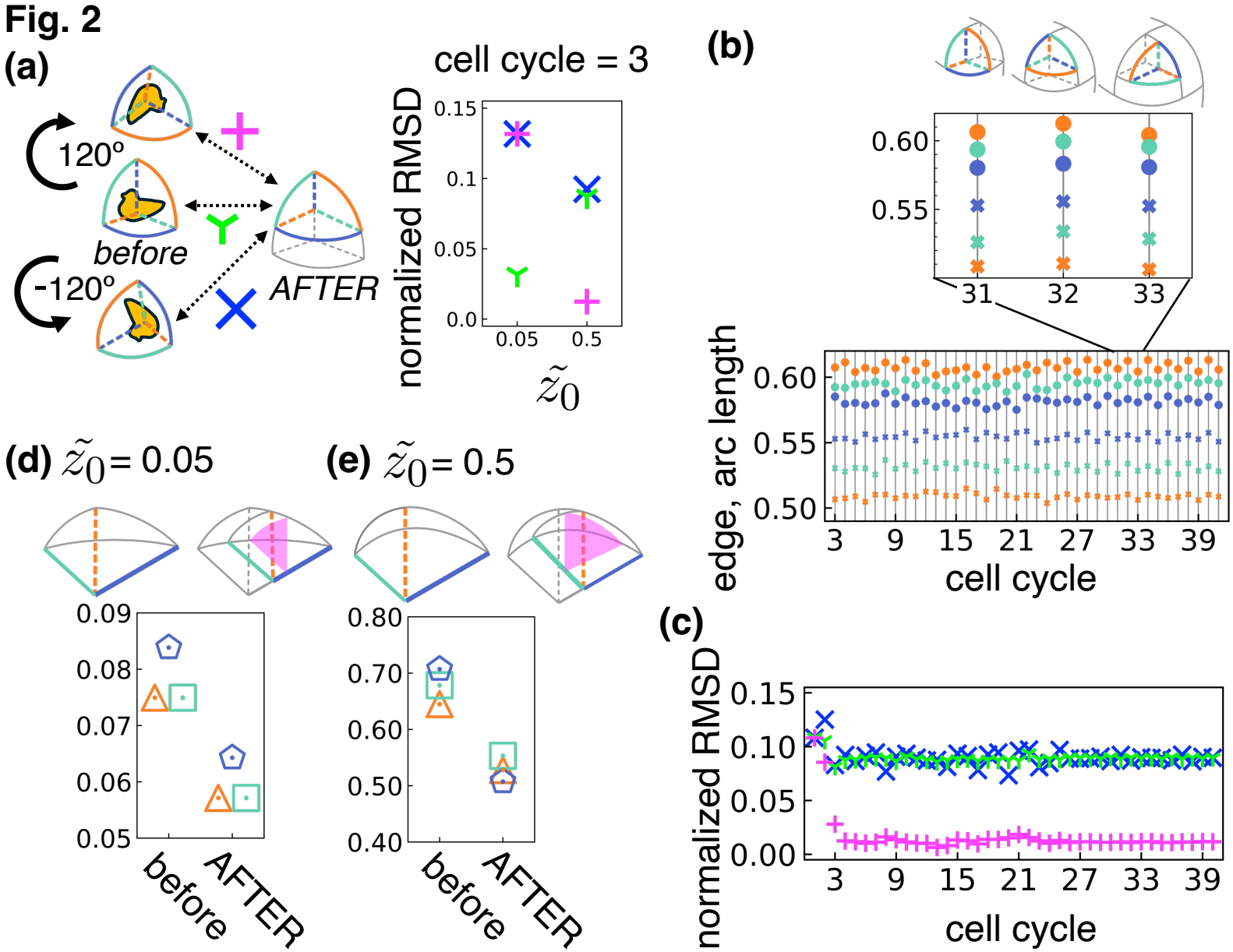

Fig. 2

Geometrical analysis of rotational divisions.

(a) Root-mean-square deviation (RMSD) between the AC outline before and after cell division was calculated by $\sqrt{\Sigma_i^3\{(S_i - s_i)^2 + (L_i - l_i)^2\}/6}$, where S_i and L_i are arc length and edge length, respectively. s_i and l_i are those after division and growth. At two different curvatures $\tilde{z}_0$ (right panel), RMSD was measured for three configurations (left panel): parallel (green Y), rotated (magenta plus), and reversely rotated (blue cross), then normalized by the typical length scale of AC (AC volume)^(1/3).

(b, c) Time course of edges and arcs of AC outline length (b) and RMSD (c) at $\tilde{z}_0 = 0.5$. The arcs and the edges are colored by the age of the adjacent and opposite merophytes, respectively (orange: M0, green: M1, and blue: M2).

(d, e) The edge length of the AC outline before and after the division at $\tilde{z}_0 = 0.05$ (d) and $\tilde{z}_0 = 0.5$ (e). θ_0 is set to 50° .

Fig. 3

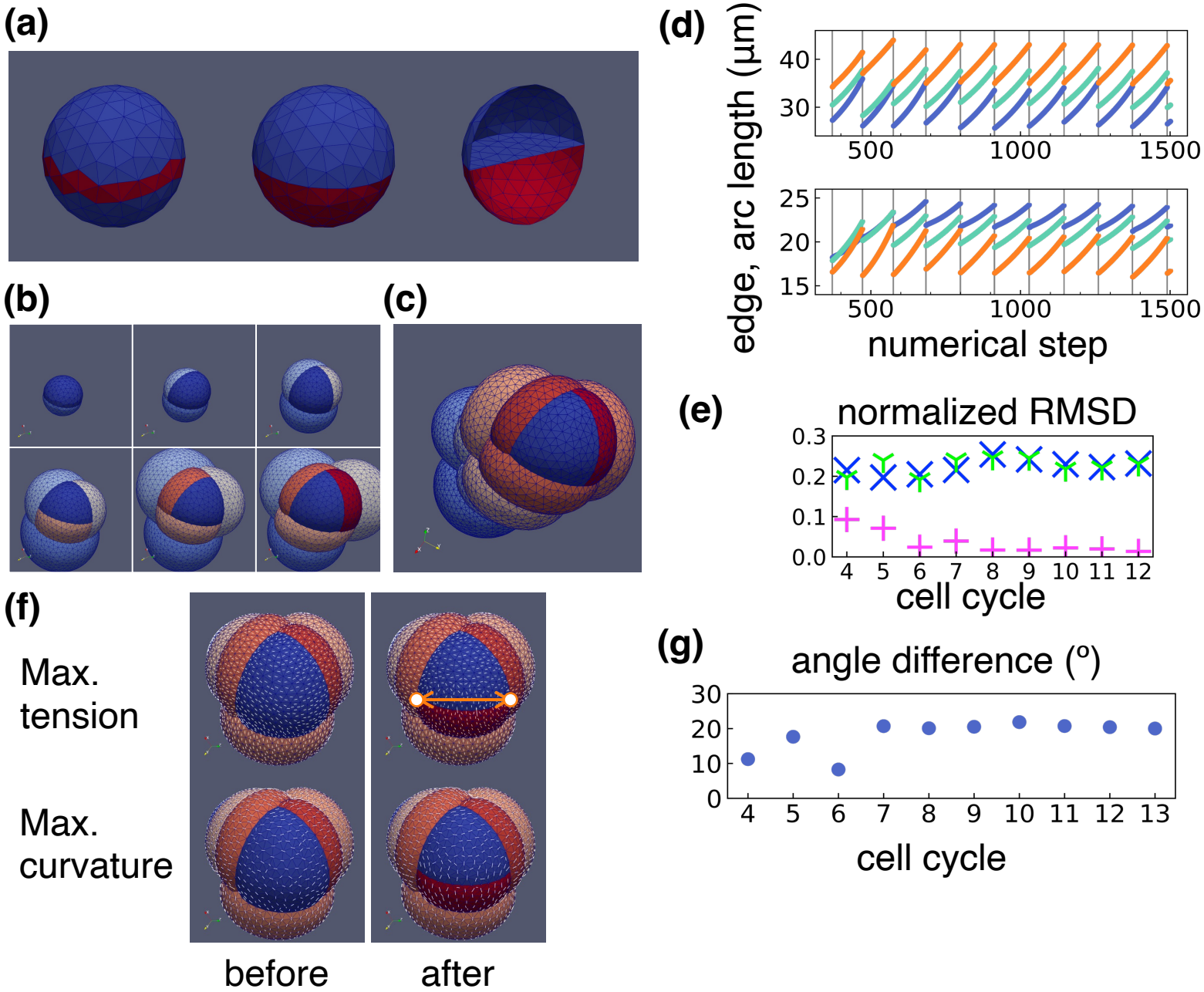

Fig. 3

Rotational divisions based on the least area rule in the mechanical model.

(a) Outline method of a cell division: detecting the triangular meshes that the division wall crosses (left) and remeshing these meshes (center). The sectional view (right). The cell wall is expressed as triangular elements.

(b) Snapshots of repetitive least area divisions of AC (colored by deep blue). Three morphologically symmetric cell divisions (top row) and subsequent asymmetric-rotational divisions (bottom row). (c) Snapshot after 12 cell divisions.

(d, e) Time course of edges, arcs (d) and RMSD (e). Colors and markers are identical to those used in Fig. 2b and 2c, respectively.

(f) The maximal tension axis (top row) and maximal curvature axis (bottom) of each triangular element just before (left column) and after (right) the least area division.

(g) Angle difference between the mean maximal tension axis and the division wall tangential (measured as the vector from AC-M0-M1 shared vertex to AC-M0-M2 shared vertex on the free surface, represented as orange two-way arrow in (f)). The radius of the initial spherical cell is 10 μm. Turgor pressure P = 0.2 MPa, Young's modulus Y = 100 MPa, Poisson's ratio σ = 0.2.

Fig. 4

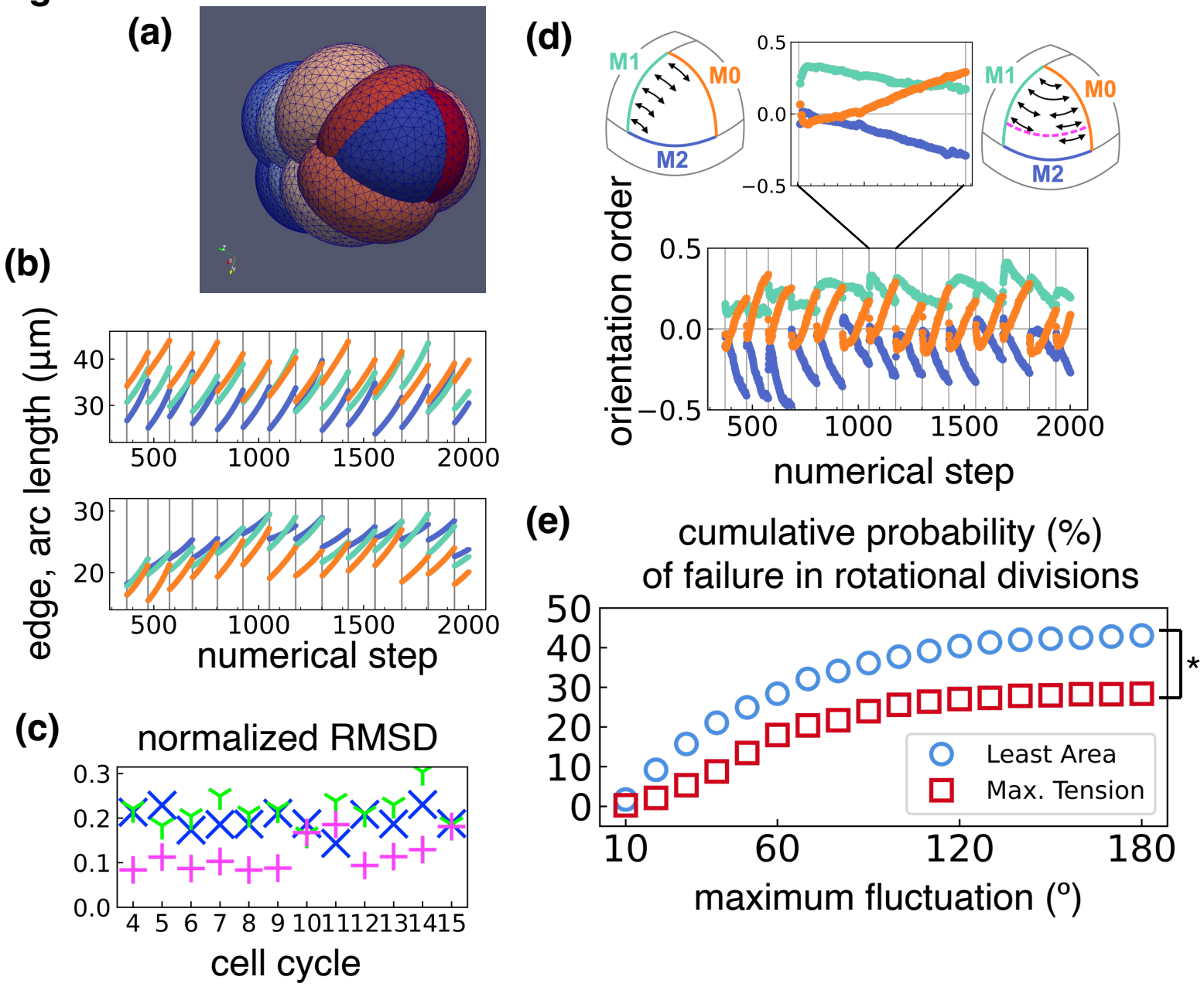

Fig. 4
Rotational divisions based on the maximal tension rule.
(a) Snapshot after 12 cell divisions.
(b, c) Time course of AC outline elements (b) and RMSD (c). Colors and markers in (b, c) are identical to those used in Fig. 2b and 2c, respectively.
(d) Bottom: Orientation order of the maximal tension axes on the AC free surface against each orthogonal axis of the AC-merophyte shared wall (AC-M0: orange, AC-M1: green, and AC-M2: blue) calculated by $\sum_i (1/2) a_i (3\cos^2(\theta_i) - 1) / \sum a_i$, where a_i and θ_i denote the area of triangle face *i* and the angle between the shared wall normal axis and the maximal tension axis, respectively. Top: Typical pattern of the maximal tension (black two-way arrows) on the AC free surface. Future division wall is represented as magenta dashed line.
(e) The cumulative probability of failure of rotational divisions under fluctuation on the division axis is compared between the least area rule and the maximal tension rule. The parameters used are those shown in Fig. 3. *p-value < 0.001 (Kolmogorov–Smirnov test).